

BelSAR : the first Belgian airborne campaign for L-band, full polarimetric bistatic and interferometric SAR acquisitions over an agricultural site in Belgium

Anne Orban^a, Denis Defrère^a, Christian Barbier^a

^a Centre Spatial de Liège, Avenue du Pré-Aily 4031 Angleur, Belgium

Abstract

The BelSAR airborne campaign was set up to prepare for future bistatic and interferometric SAR missions. The objective was to acquire L-band, full-polarimetric signatures by two airplanes, flying in various bistatic and interferometric geometries. The scientific scope was focused on agriculture and soil humidity, and the region of interest was part of the Belgian BELAIR HESBANIA test site, located close to Gembloux. Five campaigns took place between May and September 2018. Ground devices were deployed and ground measurements were obtained simultaneously to the imaging passes. The results will be exploited in a scientific project to be initiated in 2019.

1 Introduction

Passive receiving small satellite flying in formation with a larger, active satellite is a very promising concept in the field of bistatic SAR imagery [1].

In that context, the BelSAR project intended to carry out an airborne campaign for acquiring SAR bistatic and interferometric measurements at L-band and full polarization over a Belgian test site. This was a unique opportunity for the science community to validate the capability of active-passive satellite configurations and to ensure the performances of L-band SAR bistatic or multistatic imagery.

Emphasis was then put on interferometric coherence and Bistatic Radar Cross Section (BRCS) measurements at different timescales, with particular emphasis on agriculture and soil moisture monitoring, as well as bistatic SAR science.

Acquisitions took place over the vegetation growth season in 2018. Ground measurements were carried out simultaneously to the airborne acquisitions over agricultural surfaces composed of several fields, along the vegetation growing cycle.

The project was coordinated by the Centre Spatial de Liège (CSL) - University of Liège, with flights, data acquisition and SAR focusing organized by MetaSensing (NL). The ground measurements were performed by Belgian scientific teams from the University of Louvain-la-Neuve, the University of Gent and the Royal Military Academy. The full scientific exploitation of the collected datasets is being carried out in a follow-up project, started end 2019. Accordingly, only preliminary results of InSAR processing are presented here.

2 Test site

2.1 Area of interest

The test site is located inside the HESBANIA area, which is one of the four BELAIR Belgian supersites [2]. HESBANIA covers the rural area of Hesbaye/Haspengouw and is dedicated to agriculture and horticulture observations (Figure 1). Lots of data had already been and continue to be collected over this area from air/space (visible) and ground measurements, among other during the APEX (Airborne Prism Experiment) campaigns [2].



Figure 1 The four Belgian test sites and BelSAR selected area within HESBANIA (on Google Map/Earth)

2.1.1 Field selection

For measurement of soil and plant parameters, 10 winter wheat and 10 maize fields were selected in the area of interest. They all have more than 3-4 ha, are located in a rather flat terrain (fields slopes are no larger than 3 degrees) and are as homogeneous as possible (soil type, soil drainage, growing conditions) (Figure 2).

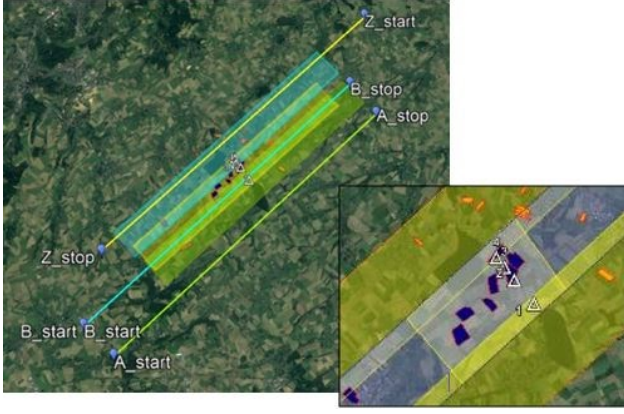


Figure 2 The full area covered by three parallel tracks in alternate directions, and the selected wheat (blue) & maize (orange) fields; subset area (track Z_s) in white.

2.1.2 Corner reflectors.

The corner reflectors (CR) are used for monostatic acquisitions to produce a geometrical reference as well as for providing the Point Spread Function (PSF) which gives the achieved resolutions together with an indication about the quality of the synchronization between the transmitter and the receiver. Four triangular pyramidal CR were deployed on the fields (Figure 3) and correctly oriented for each flight.



Figure 3 One of the four corner reflectors.

3 Flight hardware

The used L-band SAR system was developed by Meta-Sensing [4]. It is a versatile compact sensor providing imaging with spatial resolution up to one meter. A squared and a rectangular antennas were used. Common characteristics include 1.2-1.35 GHz operating frequency range, dual (V & H) linear polarization, beamwidth of 40 degrees in elevation.

The aircraft provider was a Belgian parachuting company, Skydive Spa, based at the Aerodrome of Spa – La Sauvenière, Belgium. This was the base for all airborne operations during the BelSAR campaign. Two Cessna 208 Grand Caravan were adapted and used for the five flights.

4 Data acquisition

The flights were conducted with the two airplanes flying along three parallel tracks (A, Z, B) for covering the whole scene, once in across-track (XT) configuration and once in along-track (AT) scenario. A short data sample (short track Z_s) was also acquired on a selected subset incorporating the most numerous and representative fields (maize and winter wheat) and the four corner reflectors (Figure 2). The parallel tracks were acquired in alternate directions (S-W to N-E for A and B, N-E to S-W for Z and Z_s).

The authorized bandwidth allocated by the Belgian Institute for Post and Telecommunications (BIPT) was restricted to 50 MHz centred on 1.375GHz. The PRF was 1004 Hz and the sampling frequency was 50 MHz. The flight level was either FL60 or FL70.

A preliminary study had shown that, accounting for the authorized frequency bandwidth and altitude, the orthogonal baseline for XT acquisitions should be kept around 30 meters, for preventing geometric decorrelation. In the case of along-track configuration, the AT baseline constraints were dictated by the need for azimuthal spectra superposition, which imposed an AT baseline of about $\frac{1}{4}$ of the flight altitude. The actual flight values finally were a XT baseline of about 30 meters and a AT baseline around 300 meters, except for the 1st flight where we had about 600 meters. The main drawback of these small baselines, combined with the fact that both planes are left-looking, is the resulting small bistatic angle between the transmitting and the receiving antennas, mostly in across track but also in along track configurations.

4.1 SAR data acquisition

For each flight, data from monostatic and bistatic configurations were acquired in both XT and AT geometries and for the four polarization channels HH, HV, VH and VV. Table 1 lists the flight dates and average altitudes. The boresight look angle was 45 degrees with local incidence angles in the swath between 30 and 60 degrees.

Flight #	Date of flight	Average Flight Level H_{mst} [m]
M1	30/05/2018	2100
M2	20/06/2018	2310
M3	30/07/2018	2310
M4	28/08/2018	2280
M5	10/09/2018	2330

Table 1 Dates and average flight levels of the five BelSAR flights.

4.2 Ground measurements

Soil moisture was monitored using Time Domain Reflectometry (TDR) in the top 11 cm soil layer, for at least 10 locations per field (if feasible) and, at each location, as the average of three repetitions taken within a one-meter diameter circle. Bulk density was sampled during flight 1, on all

fields, using Kopecky rings, allowing to determine field averages and standard deviations. Soil roughness was determined using a 1-m pin profilometer, with a spacing of 1 cm. The dataset for vegetation study consists in a series of properties of the crop canopy for 10 winter wheat and 10 maize fields measured concurrently to the five aircraft overpasses: plant development stage (following BBCH codification), canopy cover fraction (by Digital Hemispheric Picture), plant height, sowing density, fresh and dry biomass.

5 Preliminary results

The SAR images were obtained with a slant range resolution of 3 meter. The release of the data provided by MetaSensing consisted of 320 NetCDF files in ground range geometry with a ground resolution of 1 meter. The images are sigma Single-Look Complex (SLC) and coregistered, based on the absolute position accuracy of the navigation data, which is around 0.75 meter (less than pixel size). A composite polarimetric SAR amplitude image from flight M2, where red, green and blue respectively correspond to VV, HV and HH polarizations, is shown on Figure 4, as provided by the processor developed at the Centre Spatial de Liège. The corner reflectors appear as bright spots (see yellow arrows). Also visible as bright spots are the wind plants.

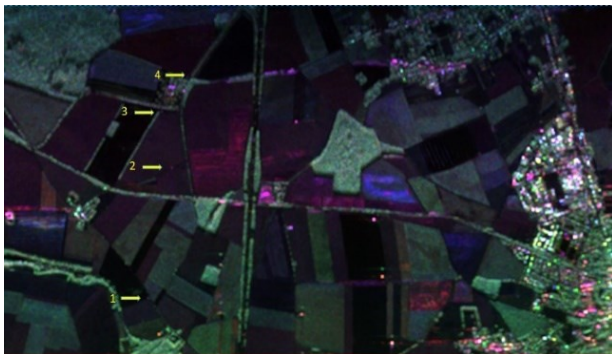


Figure 4 Polarimetric SAR image composite from flight M3, showing the CRs (yellow arrows); red: VV; green: VV; blue: VH.

Amplitude is shown in Figure 5 for the four polarization channels, in AT bistatic (slave) acquisition, for flight M4.

5.1 InSAR processing

The present paragraph describes the processing tools developed for InSAR processing, illustrates the results with specific examples and briefly discusses the origin of the coherence loss observed in several interferometric pairs. Data processing was performed using a Python code developed at CSL specifically for this project, that reads the images and metadata, performs a global coregistration, crops the master and slave images to match each other, performs Gaussian filtering, and computes a series of outputs relevant for diagnostics and InSAR analysis. Further to am-

plitude images (Fig. 4 and 5) and coordinate maps (in latitude, longitude and height), the software generates the incidence angles for both master and slave files, the bistatic angle, and the Digital Elevation Model (Figure 6). Then, the interferometric products are generated: coherence map, interferogram and phase maps.



Figure 5 Amplitude images of bistatic acquisition in the 4 polarization channels, flight M4. From top left to bottom right: HH, HV, VH and VV.

It is well established that the level of coherence depends on several factors, among which the geometric decorrelation (g), which is known to occur as the separation between the two plane trajectories increases: $g = 1-b/b$, where b is the perpendicular baseline and b the critical baseline. The perpendicular baseline and geometric decorrelation maps are also evaluated by the code. The latest version is fully automatized in order to process all the interferometric pairs efficiently (e.g., 80 image pairs for a given master acquisition, accounting for the four tracks and polarizations).

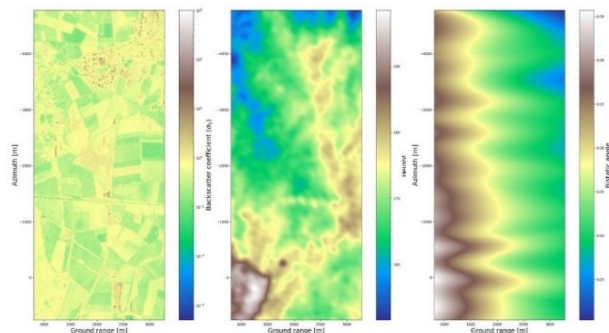


Figure 6 Amplitude image (left), DEM (center) and Bistatic angle (right) for pair M55, AT, HH pol.

As already said, constraints were imposed to limits the baselines to small value in order to preserve coherence, which consequently reduces the bistatic angle, especially for XT configuration. However, despite the small geometric baselines, coherence extracted from single-pass bistatic pairs is usually rather poor across the image. The coherence map and interferometric phase are shown on Figure 7, together with geometric decorrelation, for the pair M55, along-track (AT), short track, HH polarization. Similar results are obtained for the XT geometry. For monostatic repeat pass acquisitions, acquired with about one month temporal baseline, coherence losses are considerable, making these im-

age pairs taken temporally far apart hardly usable for scientific exploitation. This clearly appears in Figure 8, showing the monostatic repeat-pass coherence maps computed with the acquisition of flight 5 (M5) as master image and the corresponding acquisitions of the other flights (M1 to M4) as slave images, for the XT geometry and VV polarization. The observation of the coherence maps shows very strong coherence losses between the different missions, resulting from the combination of temporal effects and geometric decorrelation due to the relatively large perpendicular baseline, accounting for flight altitude and signal bandwidth (50MHz).

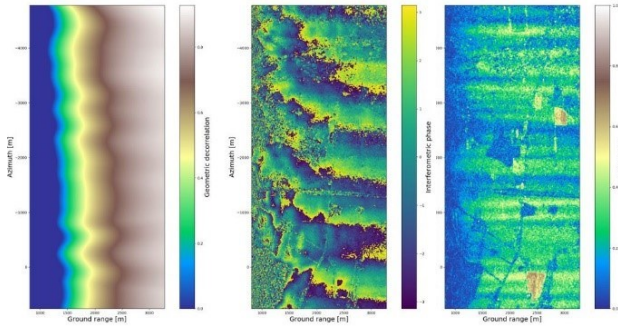


Figure 7 Geometric Decorrelation (left), Interferogram (center) and Bistatic Coherence map (right), pair M55, AT, HH pol.

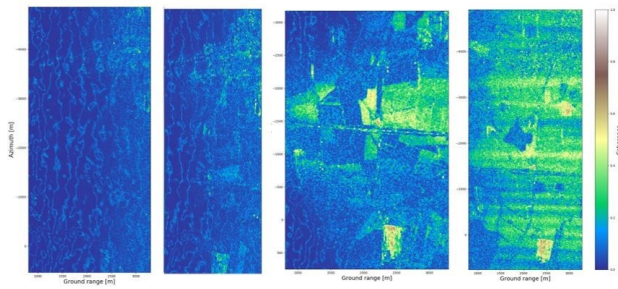


Figure 8 Coherence maps for flight M5 as master and flights M1 to M4 (from left to right) as slave images, illustrating strong temporal coherence loss (XT, polarization VV).

However, other factors clearly contribute to degrade the interferometric coherence. In bistatic configuration, using two different clocks for the transmitter and receiver systems can result in a lack of synchronization, compared with a monostatic configuration where the unique transmitter/receiver system operates with absolute time and phase references. Consequences are positioning and phase errors in the output SLC images, giving rise to azimuthal fringes in the interferogram. Implementing a synchronization algorithm should allow to evaluate and correct this clock phase error. Coherence should also be improved by implementing fine-patch coregistration, then reducing residual airplane motion effects.

6 Conclusion

The BelSAR Campaign was conducted in spring and summer 2018. The targeted application fields were soil moisture, agriculture and bistatic SAR science. Five air-borne missions allowed to acquire L-band multi-temporal bistatic full-polarimetric SAR data. The data were acquired with two airplanes flying in both along-track and across-track interferometric configurations over an area being part of the HESBANIA Belgian BELAIR supersite.

In-situ ground measurements were done simultaneously or within a few days from each airborne mission, to get information on soil roughness and moisture, as well as crop canopy properties in wheat and maize fields

The SAR data were successfully processed. An automatic software was developed to generate the interferometric products. Small baselines were imposed based on coherence requirements, the main drawback on the data set being the small bistatic angle between the transmitting and the receiving antenna both in along-track and across-track configurations. Despite these small baselines, even the resulting coherence extracted from double-pass monostatic pairs is rather poor across the images. A following project, under the name BelSAR_Science, has kicked off at the end 2019 for a detailed scientific exploitation of the L-band SAR bistatic and in situ data. Further to soil moisture retrieval and agriculture monitoring, it would be particularly useful to optimize the coherence by implementing fine patched-based coregistration to minimize the impact of the residual motion of the airplanes, and by reducing synchronization defaults, by clock phase error correction.

7 Literature

- [1] G. Krieger and A. Moreira, Spaceborne Bi- and Multistatic SAR: Potential Challenges, IEEE Proceedings - Radar Sonar and Navigation 153(2006-06).
- [2] <https://eo.belspo.be/en/belair>
- [3] <https://apex-esa.org/en/campaigns>
- [4] I. Hendriks, A. Meta, C. Trampuz, A. Coccia, S. Placidi, M. Davidson, and D. Schuettemeyer, MetaSensing's Novel L-Band Airborne SAR Sensors for the BelSAR Project: First Results, Advanced RF Sensors and Remote Sensing Instruments Conference 2017

8 Acknowledgement

This campaign was carried out under ESA Contract 4000117154/16/NL/FF/mc.